

Optical Engineering

SPIEDigitalLibrary.org/oe

Accurate wavelength calibration method using system parameters for grating spectrometers

Kang Liu
Feihong Yu



SPIE

Accurate wavelength calibration method using system parameters for grating spectrometers

Kang Liu
Feihong Yu
Zhejiang University
Optical Engineering Department
Hangzhou 310027, China
E-mail: feihong@zju.edu.cn

Abstract. In this paper, an accurate method is proposed for wavelength calibration in grating spectrometers. The analytical calibration model of the Czerny–Turner optical system, which describes the relationship between the wavelengths and the pixel numbers with function of the system parameters, is established on the basis of the grating equation and geometric optics. An optimization fitting algorithm is introduced to calculate the practical system parameter values in this model. Experimental tests are conducted in our manufactured spectrometer. The results show that this method has higher calibration accuracy in a broadband spectrometer system and less dependence on the spectral lines chosen compared to the traditional polynomial method. This novel wavelength calibration method also can be applied to other plane-grating or concave-grating spectrometers. © The Authors. Published by SPIE under a Creative Commons Attribution 3.0 Unported License. Distribution or reproduction of this work in whole or in part requires full attribution of the original publication, including its DOI. [DOI: 10.1117/1.OE.52.1.013603]

Subject terms: grating spectrometer; wavelength calibration; geometric optics; system parameters.

Paper 121216 received Aug. 23, 2012; revised manuscript received Dec. 12, 2012; accepted for publication Dec. 12, 2012; published online Jan. 7, 2013.

1 Introduction

Grating spectrometers disperse lights with grating while recording the spectrum with a one-dimensional (1-D) photo-diode array (PDA) or charge-coupled device (CCD). The resolution of the spectrometer is determined by the entrance slit, the grating groove density, the imaging mirror focal length, and the pixel width of the array detector.^{1,2} Each pixel of the detector corresponds to a specific wavelength, which is limited by the resolution.² The relationship between the pixels and the wavelengths should be established by the approach called wavelength calibration.³

Four kinds of wavelength standard are commonly used to calibrate the spectrometers, such as emission lines from deuterium lamp, emission lines from mercury lamp, transmission lines from holmium oxide with didymium filters, and 4% holmium oxide in 10% perchloric acid.⁴ However, the most convenient process is to use the standard mercury–argon light source with known wavelengths of spectral lines.⁵ In conventional analysis, the relationship between the wavelengths and the pixels is expressed by a polynomial with appropriate coefficients.^{6–8} The accuracy of the polynomial fitting method is lowered when interpolation or extrapolation is used for the wavelengths distant from the standard lines. It means that the selection and distribution of the standard lines restrict the calibration accuracy. Youngquist et al.⁹ utilized the spectrally resolved white-light interferometry by creating equidistant calibration lines. Perret et al.¹⁰ used a Fabry–Perot reference filter (FRT) to create equidistant calibration lines with similar peak intensities where the calibration lines are rare in some wavelength range. These approaches improve the calibration accuracy of the polynomial fitting method. In addition, the bandwidth of the spectrometer also limits calibration accuracy. Martinsen et al.¹¹ used a monochromator to filter the calibration source so that each calibration line

could be measured separately. The wavelength calibration accuracy is significant in the spectrum measurement but is limited by the above aspects.

In this paper, an accurate wavelength calibration method using the optical system parameters is introduced to thoroughly address the above calibration issues. The analytical model of the relationship between wavelengths and pixels with the optical system parameters is established on the basis of geometric optics. An optimization algorithm is used to solve the practical system parameters with a specific merit function. To test and verify the calibration method, a Czerny–Turner spectrometer is designed and manufactured. The calibration results of the method in our spectrometer show that the wavelength deviations on each pixel are reduced apparently in the whole wavelength range compared to the conventional method. Meanwhile, the novel calibration method shows no dependence on the selection of the calibration standard lines. Furthermore, the calibration method is flexible in that it is also suitable to other plane- or concave-grating spectrometers.

2 Calibration Method Using System Parameters

2.1 Calibration Model

The Czerny–Turner structure is the most popular commercial portable spectrometer system. Figure 1 shows the two-dimensional (2-D) schematic diagram of the Czerny–Turner spectrometer. The slit light source S , which is an approximate line source, is located at the front focal plane of the collimating mirror. S emits divergent rays onto the collimating mirror with the coupled numerical aperture. As the collimating spherical mirror tilts a tiny angle, the collimated light reflects onto the plane grating. The grating disperses the polychromatic light into monochrome rays with different emergence angles. Then the imaging mirror focuses these

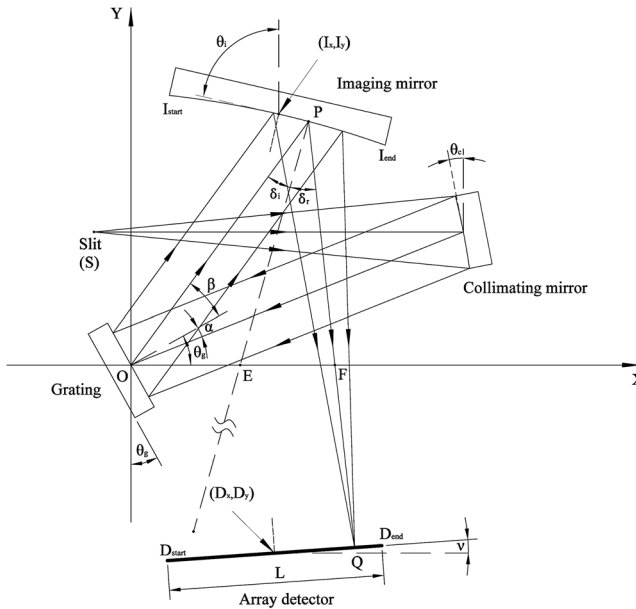


Fig. 1 Schematic diagram of the Czerny–Turner spectrometer.

monochrome rays onto the target surface of the array detector. So the light intensity on each pixel, actually, is the image of the slit S of a specific wavelength with some spread width caused by the system aberration. This is the basic principle of the so-called linear detector grating spectrometer.

As shown in Fig. 1, we establish the Cartesian coordinate system with the unit of millimeter. The midpoint of the grating groove surface is considered as the origin marked with O . According to the geometric optics theory, the incident angle of the collimated light on the grating groove can be expressed as $\alpha = \theta_g - 2\theta_c$. The grating diffraction equation can be given as

$$\sin \alpha - \sin \beta = nm\lambda. \quad (1)$$

In Eq. (1), n is the nominal groove density, and m is the diffraction order. α and β denote the incident angle and diffraction angle on the plane-grating groove. They are located at the different sides of the grating normal, respectively. Hence, we have

$$\beta = \arcsin[nm\lambda + \sin(\theta_g - 2\theta_c)]. \quad (2)$$

The diffraction ray with angle β diffracted from point O hits the imaging mirror at point P . With the analytic geometry theory, the straight line equation of line OP in the coordinate system can be expressed as

$$y = \tan(\beta + \theta_g)x, \quad (3)$$

where x denotes the independent variable and y denotes function value of the straight line equation. Similarly, the curve equation of the spherical imaging mirror surface $I_{\text{start}}I_{\text{end}}$ can be expressed as

$$(x - C_x)^2 + (y - C_y)^2 = R^2, \quad (4)$$

where $(C_x, C_y) = (I_x - R \cos \theta_i, I_y - R \sin \theta_i)$ is the circle center coordinate of the imaging spherical mirror C . $((I_x, I_y)$, denotes the midpoint of the imaging spherical mirror surface (curve $I_{\text{start}}I_{\text{end}}$), and R denotes the imaging mirror spherical radius. Then we have the simultaneous equations of the diffraction ray (OP) and the imaging spherical mirror surface ($I_{\text{start}}I_{\text{end}}$) listed below:

$$\begin{cases} y = \tan(\beta + \theta_g)x \\ (x - I_x + R \cos \theta_i)^2 + (y - I_y + R \sin \theta_i)^2 = R^2 \end{cases}. \quad (5)$$

The solution of Eq. (5) is the coordinate of point $P(P_x, P_y)$.

$$\begin{aligned} P_x &= x = \frac{1}{\tan^2(\beta + \theta_g) + 1} \cdot [I_x - R \cos \theta_i + \tan(\beta + \theta_g)(I_y - R \sin \theta_i)] \\ &\quad + \{\tan^2(\beta + \theta_g)[R^2 - (I_x - R \cos \theta_i)^2] + 2 \tan^2(\beta + \theta_g)(I_x - R \cos \theta_i)(I_y - R \sin \theta_i) - (I_y - R \sin \theta_i)^2 + R^2\}^{\frac{1}{2}} \\ P_y &= y = \frac{\tan(\beta + \theta_g)}{\tan^2(\beta + \theta_g) + 1} \cdot [I_x - R \cos \theta_i + \tan(\beta + \theta_g)(I_y - R \sin \theta_i)] \\ &\quad + \{\tan^2(\beta + \theta_g)[R^2 - (I_x - R \cos \theta_i)^2] + 2 \tan^2(\beta + \theta_g)(I_x - R \cos \theta_i)(I_y - R \sin \theta_i) - (I_y - R \sin \theta_i)^2 + R^2\}^{\frac{1}{2}}. \end{aligned} \quad (6)$$

On the imaging mirror surface, the incident ray (OP) and the reflected ray (PQ) follow the reflection law, which indicates that the reflection angle δ_r is equal to the incident angle δ_i . The normal line passing point P intersects the x -axis at point E . With the coordinates of point P and circle center C , the slope of line PE can be expressed as $(\frac{P_y - I_y + R \sin \theta_i}{P_x - I_x + R \cos \theta_i})$. So with the trigonometric calculation in triangle OPE , we have

$$\delta_r = \delta_i = \arctan\left(\frac{P_y - I_y + R \sin \theta_i}{P_x - I_x + R \cos \theta_i}\right) - (\beta + \theta_g). \quad (7)$$

The reflected ray (PQ) emits along with the emergent angle δ_r . It hits the array detector surface at point Q and intersects the x -axis at point F . With the trigonometric

relationship in triangle OPF , the slope k of line PQ can be expressed as $k = \tan(\pi - 2 \arctan \frac{P_y - I_y + R \sin \theta_i}{P_x - I_x + R \cos \theta_i} + \beta + \theta_g)$. Combining the straight line equation of line PQ and the straight line equation of the detector surface $(D_{\text{start}}, D_{\text{end}})$ yields:

$$\begin{cases} y = -kx + P_y + k \cdot P_x \\ y = \tan \nu x + D_y - D_x \tan \nu \end{cases}. \quad (8)$$

where (D_x, D_y) denotes the midpoint coordinate of the array detector, and ν denotes the tilt angle between the target surface and x -axis. The coordinate of Q can be obtained by solving Eq. (8):

$$(Q_x, Q_y) = \left(\frac{P_y + k \cdot P_x + D_x \tan \nu - D_y}{\tan \nu + k}, -k \cdot \frac{P_x + k \cdot P_x + D_x \tan \nu - D_y}{\tan \nu + k} + P_y + k \cdot P_x \right). \quad (9)$$

Considering the practical spectrometer system, the coordinate of Q should be transformed into the pixel number of the array detector. The relationship between the pixel numbers and the relative coordinates can be represented as

$$\begin{cases} D_x + \left(\frac{N}{2} - i\right) \cdot \Delta \cdot \cos \nu \leq Q_x \leq D_x + \left(\frac{N+1}{2} - i\right) \cdot \Delta \cdot \cos \nu \\ D_y + \left(\frac{N}{2} - i\right) \cdot \Delta \cdot \sin \nu \leq Q_y \leq D_y + \left(\frac{N+1}{2} - i\right) \cdot \Delta \cdot \sin \nu \end{cases}, \\ i = (0, 1, 2, \dots, N). \quad (10)$$

where N is the total pixel number of the detector, i denotes the i 'th pixel, and Δ is the pixel width. Each pixel of the array detector corresponds to a coordinate interval in the calibration model.

Combining Eqs. (2), (9), and (10), the wavelength calibration model can be denoted as

$$\lambda_i = f(\theta_c, \theta_i, \theta_g, I_x, I_y, D_x, D_y, \nu; i). \quad (11)$$

It means that the wavelength λ_i on the i th pixel corresponds to the tilt angle of the collimated mirror (θ_c), the tilt angle of the grating (θ_g), the relative center position and the tilt angle of the imaging mirror (I_x, I_y, θ_i), the relative center position and the tilt angel of the detector (D_x, D_y, ν). Briefly, the relationship between the wavelengths and the pixel numbers is a function of the spectrometer system parameters. The tolerance analysis of the spectrometer design shows that machining errors have little effect on the imaging quality. So in the calibration model, the machining errors of the optical elements of the mirrors and the grating are not considered. As a matter of fact, these machining errors and the assembly errors can be compensated for when the imaging surface is aligned.

2.2 Parameter Fitting Solution

With the practical alignment of the Czerny–Turner spectrometer system, the positions and the tilt angles are fixed for the collimating mirror and imaging mirror. The plane grating can be rotated freely along its axis O . The relative position and the tilt angle of the array detector are adjustable. So the parameters $\theta_c, \theta_i, I_x, I_y$ are fixed after the spectrometer is assembled, and parameters θ_g, D_x, D_y, ν are regulatable. The wavelength calibration model can be simplified as

$$\lambda_i = f(\theta_g, D_x, D_y, \nu; i). \quad (12)$$

The wavelength calibration can be accomplished when the four parameters are determined. However, solving Eq. (12) with four known wavelength–pixel pairs is not feasible because the four simultaneous equations are nonlinear. According to our experience in spectrometer alignment, the practical values of the four parameters do inevitably approximate at the design values of the spectrometer. So the

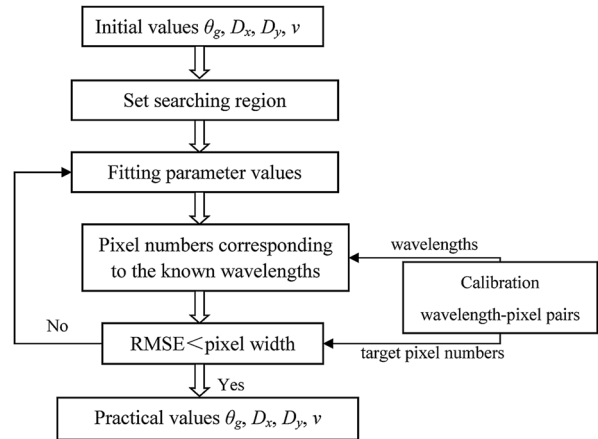


Fig. 2 Flow diagram for iterative parameters solution.

downhill simplex algorithm can be used¹² to optimize the four practical parameters. The flow diagram of the downhill simplex optimization algorithm is depicted in Fig. 2.

At first, the original design values θ_g, D_x, D_y, ν are set as the initial values. Then the searching space is determined by the experience of spectrometer alignment. With the calibration light source, the standard peak wavelengths and their positions on the CCD detector are obtained. Then the pixel coordinates (x_{f_i}, y_{f_i}) of the known wavelengths can be calculated with the fitting parameter values using Eq. (12). The practical pixel coordinates (x_{p_i}, y_{p_i}) are obtained by taking out the pixel numbers using Eq. (10). To identify the best fit, the merit function is represented by a root mean square error (RMSE), which is defined by

Table 1 Spectrometer parameters.

Parameter	Value
R	130 mm
n	600 lines/mm
m	-1
Slit width	25 μm
θ_c	11 deg
θ_i	77 deg
θ_g	29.1 deg
I_x	20 mm
I_y	34 mm
D_x	19.44 mm
D_y	-25.50 mm
ν	4 deg

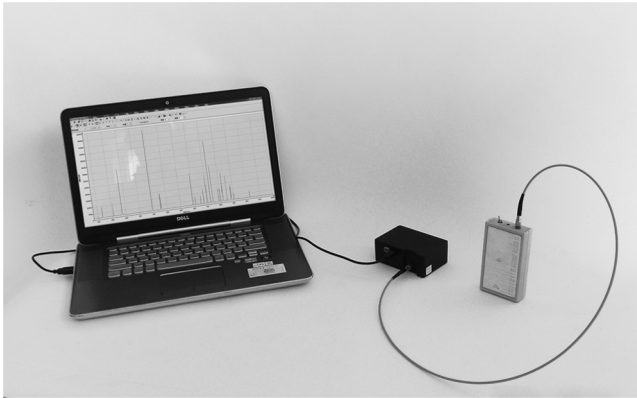


Fig. 3 Photograph of the calibration system.

$$\text{RMSE} = \frac{1}{n} \sum_{i=1}^n [(x_{f_i} - x_{p_i})^2 + (y_{f_i} - y_{p_i})^2]^{\frac{1}{2}}, \quad (13)$$

where n denotes the number of the calibration wavelength-pixel pairs that participate in the wavelength calibration. The RMSE represents the average deviation between the fitting pixel coordinates and the practical pixel coordinates. Minimizing the RMSE value allows us to obtain the best fitting parameters. In the spectrometer system, the best fit is considered if this deviation is less than the pixel width of the detector. It means that the fitting pixel coordinates are in the coordinate intervals of the practical pixel according to Eq. (10). With the best optimized fit at the pixel coordinates, the fitting parameters θ_g , D_x , D_y , ν are used to calculate each wavelength value of each pixel on the detector with Eqs. (10) and (12). The searching region should be adjusted when the best fit cannot be obtained, and the optimization should be operated again.

3 Results and Discussion

A Czerny–Turner optical system is designed and manufactured to verify the wavelength calibration method using

system parameters. The designed Czerny–Turner system parameters are shown in Table 1.

The values of I_x , I_y , D_x , D_y are the relative positions in the coordinate system, which is described in Sec. 2. A linear array CCD chip (Toshiba TCD1304DG) with 3648 pixels, 8 μm pitch width (Δ), is used to record the dispersed spectrum simultaneously. The designed wavelength range is from 330 to 1000 nm. The practical available wavelength range would be slightly different because of the alignment deviation. The spectral resolution is better than 0.5 nm at the central wavelength and up to 2 nm at the edge wavelengths.

A mercury–argon calibration light source (HG-1, Ocean Optics) is chosen as the wavelength calibration standard. The experiment system is shown in Fig. 3, and the actual mercury–argon spectrum recorded by our spectrometer is shown in Fig. 4. The values marked on the peaks with the units of nanometer are wavelengths of the mercury–argon spectral lines.¹³ In the conventional grating spectrometer systems, the first-order spectra carry the primary diffraction intensity of the grating. So only the first-order spectra need to be recorded by the array detector. The existence of the high-order spectra would affect the distribution of the desired spectra. As is seen in Fig. 3, high-order spectra in our spectrometer are eliminated by the dedicated order-sorting filter.¹⁴

The pixel positions of each peak are determined by apodization procedure.⁵ As no CCD subdivision¹⁵ is done, the available wavelengths of the mercury–argon lines and their corresponding integer pixel numbers are shown in Table 2.

The values of the spectrometer system parameters listed in Table 1 are substituted into the wavelength calibration model [Eq. (10)], except that θ_g , D_x , D_y , ν are used as the initial values in the parameter fitting solution. The wavelength-pixel pairs shown in Table 2 are selectively chosen to calculate the best fitting parameter values of θ_g , D_x , D_y , ν . To achieve a better optimization result, six spectral lines (365.015, 435.833, 546.074, 696.543, 763.511, and

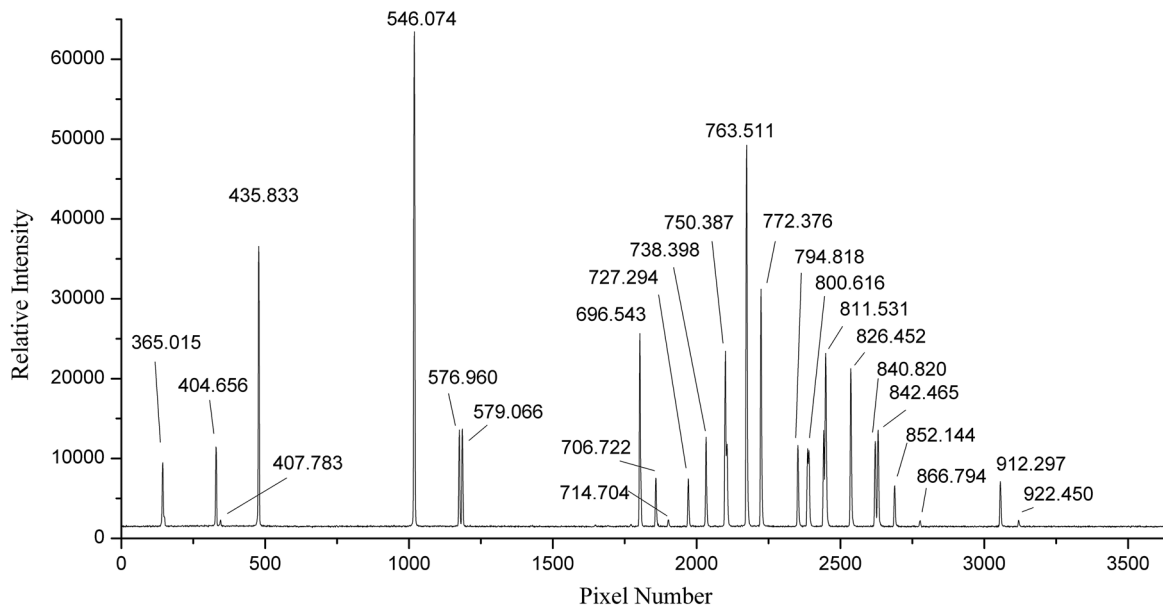


Fig. 4 Spectrum of the mercury–argon calibration light source.

Table 2 Pixel positions of the spectral lines.

Line wavelength (nm)	Position (pixel number)	Line wavelength (nm)	Position (pixel number)
365.015	144	750.387	2100
404.656	329	763.511	2174
407.783	345	772.376	2224
435.833	478	794.818	2352
546.074	1019	800.616	2386
576.960	1175	811.531	2449
579.066	1186	826.452	2536
696.543	1803	840.820	2621
706.722	1858	842.465	2631
714.704	1903	852.144	2689
727.294	1971	866.794	2777
738.398	2033	912.297	3056
		922.450	3120

826.452 nm), which are disturbed almost uniformly in the whole spectrum range, are chosen as the standard lines for the wavelength calibration.

After 500 optimization cycles, the practical parameter values used in the wavelength calibration are as follows: $\theta_g = 28.76$ deg, $D_x = 22.08$ mm, $D_y = -24.116026$ mm, $\nu = 6.76$ deg, and RMSE = 0.000185 mm, which is much smaller than the pixel width. The optimized fitting parameters demonstrate that the variations of the four parameters are caused by the alignment. Then the corresponding wavelengths on each pixel can be calculated by Eqs. (10) and (12) with the best fitting values of θ_g , D_x , D_y , ν .

The wavelength calibration result using system parameters is compared with the conventional polynomial fitting method. The accuracy of the polynomial fitting calibration is limited by the order of the fitting polynomial. The six wavelength-pixel pairs above are chosen to structure the fitting five-order polynomial. The deviations between the calibrated wavelengths and the standard wavelengths are the basis to estimate the accuracy of the calibration results. So the calibrated wavelengths of the mercury–argon spectral lines are plotted, and the comparison results using the proposed method and polynomial method are shown in Fig. 5.

The deviations of the conventional polynomial method are obviously increased in the wavelength range distant from the standard calibration lines because interpolation or extrapolation is used. The calibration deviations of our parameter method could stabilize at the interval of 0.1 nm. To demonstrate the superiority of our method, six other standard spectral lines, which are not uniformly distributed in the

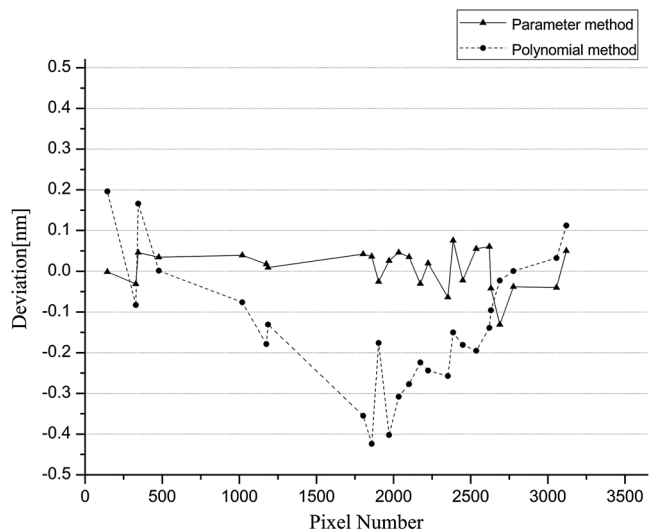


Fig. 5 Calibration deviations of parameter method and polynomial method with six uniform standard spectral lines (365.015, 435.833, 546.074, 696.543, 763.511, and 826.452 nm).

whole wavelength range, are used to calibrate the spectrometer. The comparison results are shown in Fig. 6.

The results show that the calibration deviations of the parameter method could also stabilize within a range of ± 0.25 nm. The deviations of the polynomial method increase rapidly, and the maximum deviation is > 2 nm. Similarly, the lack of standard lines in the long-wave range causes the decrease of the calibration. The comparison between the above two calibrations shows that the system parameter calibration method has higher accuracy than the polynomial fitting method. Also, the accuracy of the polynomial fitting method strongly depends not only on the selection of the standard spectral lines but also on the quantity of the chosen lines. However, deviations of our calibration method can be confined within a small region no matter which (or how many) standard spectral lines are used.

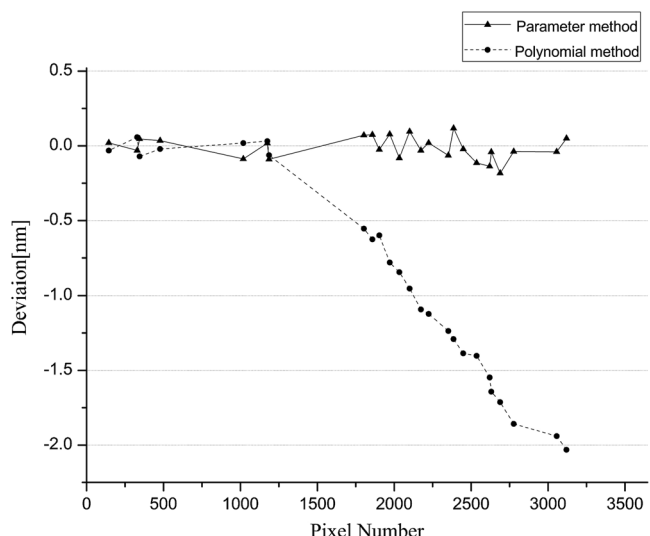


Fig. 6 Calibration deviations of parameter method and polynomial method with six nonuniform standard spectral lines (365.015, 404.656, 407.783, 435.833, 546.074, and 576.960 nm).

4 Conclusions

The wavelength calibration method using system parameters presented in this paper is the solution originating from geometric optics. The calibration model of the Czerny-Turner optical system, which exactly describes the relationship between the wavelengths and the pixel numbers, is established on the base of Cartesian coordinate system. An optimization fitting algorithm with a dedicated merit function is used to calculate the four variable system parameters in the calibration model.

A Czerny-Turner spectrometer is designed and manufactured to verify this calibration method. The calibration results show that our method has the calibrated wavelength deviation of <0.1 nm in a broadband wavelength range. With the advantages of higher accuracy and less dependence on the spectral lines selection, our calibration method performs significantly better than the traditional polynomial fitting calibration method. Also, the solved system parameters can verify the reliability of the optical system alignment. The idea of wavelength calibration using system parameters can be applied to other plane-grating or concave-grating spectrometers.

References

1. J. F. Wu, Y. Y. Chen, and T. S. Wang, "Flat field concave holographic grating with broad spectral region and moderately high resolution," *Appl. Opt.*, **51**(4), 509–514 (2012).
2. M. A. Gil, J. M. Simon, and A. N. Fantino, "Czerny-Turner spectrograph with a wide spectral range," *Appl. Opt.*, **27**(19), 4069–4072 (1988).
3. L. Bai et al., "Study on the wavelength calibration of type III concave grating spectrometry," *Chin. Opt. Lett.*, **2**(3), 174–176 (2004).
4. "Performance of UV-Vis spectrophotometer," http://www.cvg.ca/images/Performance_UV_Vis.pdf.
5. C. H. Tseng et al., "Wavelength calibration of a multichannel spectrometer," *Appl. Spectrosc.*, **47**(11), 1808–1813 (1993).
6. J. T. Brownrigg, "Wavelength calibration methods for low-resolution photodiode array spectrometers," *Appl. Spectrosc.*, **47**(7), 1007–1014 (1993).
7. S. T. Wollman and P. W. Bohn, "Evaluation of polynomial fitting functions for use with CCD arrays in Raman spectroscopy," *Appl. Spectrosc.*, **47**(1), 125–126 (1993).
8. Z. M. Xu and B. X. Yu, "Wavelength calibration for PC2000-PC/104 spectrometer," *Opt. Precision Eng.*, **12**(1), 11–14 (2004).
9. R. C. Youngquist, S. M. Simmons, and A. M. Belanger, "Spectrometer wavelength calibration using spectrally resolved white-light interferometry," *Opt. Lett.*, **35**(13), 2257–2259 (2010).
10. E. Perret, T. E. Balmer, and M. Heuberger, "Self-consistent algorithm for calibration spectrometers to picometer accuracy over the entire wavelength range," *Appl. Spectrosc.*, **64**(10), 1139–1144 (2010).
11. P. Martinsen et al., "Accurate and precise wavelength calibration for wide bandwidth array spectrometers," *Appl. Spectrosc.*, **62**(9), 1008–1012 (2008).
12. R. J. Koshel, "Enhancement of the downhill simplex method of optimization," *Proc. SPIE*, **4832**, 270–282 (2002).
13. "HG-1 Mercury Argon calibration light source," <http://www.oceanoptics.com/products/hg1.asp>.
14. K. Liu and F. H. Yu, "Research on eliminating high-order spectrum in broadband miniature spectrometer system," *Proc. SPIE*, **8415**, 841506 (2012).
15. L. J. Gu et al., "Research of the camera calibration based on digital image processing," *Proc. SPIE*, **6696**, 66961W (2007).



Kang Liu received his BS in 2007. He is now pursuing his PhD at Zhejiang University. His main research interests are spectrometer instrument design and spectrometer application system design.



Feihong Yu received his PhD from the Optical Engineering Department at Zhejiang University in 1993. His main interests are liquid crystal displays, LCD projection display, optical and digital image processing, optical instrumentation, 3-D medical image processing, and visualization. He is the author or coauthor of more than 100 technical papers.